

X-Ray Line-Shape Diagnostics and Novel Stigmatic Imaging Schemes for the National Ignition Facility

M. Bitter¹, K. W. Hill¹, N. A. Pablant¹, L. F. Delgado-Aparicio¹, P. Beiersdorfer², E. Wang², and M. Sanchez del Rio³

¹*Princeton Plasma Physics Laboratory, P. O. Box 451, Princeton, New Jersey 08543, USA*

²*Lawrence Livermore National Laboratory, 7000 East Ave, Livermore, CA 94550, USA*

³*European Synchrotron Radiation Facility, 38043 Grenoble Cedex, France*

I Introduction.

In response to a recent solicitation from the US Department of Energy we proposed the development of a new x-ray line-shape diagnostic and novel stigmatic imaging schemes for the National Ignition Facility (NIF). These diagnostics are based on the imaging properties of spherically bent crystals, explained in Fig. 1, which have already been successfully applied to the diagnosis of extended tokamak plasmas for measurements of the ion-temperature and toroidal flow-velocity profiles [United States Patent: US 6,259,763 B1] and refs. [1, 2].

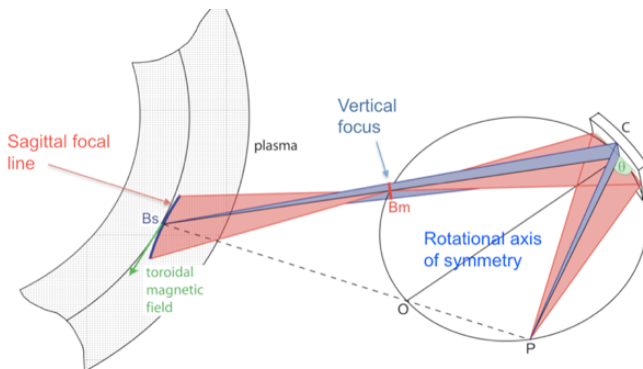


Fig. 1: Imaging properties of a spherical crystal.

A spherical crystal produces two, mutually perpendicular, meridional and sagittal, line images at B_m and B_s of point source at P , as a result of the astigmatism of a spherical mirror. Rays which emanate from a sagittal line source at B_s are, therefore, focused at P . Since the ray pattern is symmetric with respect to rotations about the normal OC

to the spherical crystal, the sagittal line source at B_s and its image at the point P move in opposite directions on a cone about OC under such an imagined rotation of the ray pattern, so that one obtains spatial resolution in a direction perpendicular to the dispersion plane. Figure 1 shows the preferred experimental arrangement on tokamaks, where the sagittal line source is parallel to the toroidal magnetic field, along which the electron density, electron temperature, and x-ray emissivity are uniform. Spatial resolution is then obtained in a direction perpendicular to the toroidal magnetic field. Figure 2 shows an example of spatially resolved

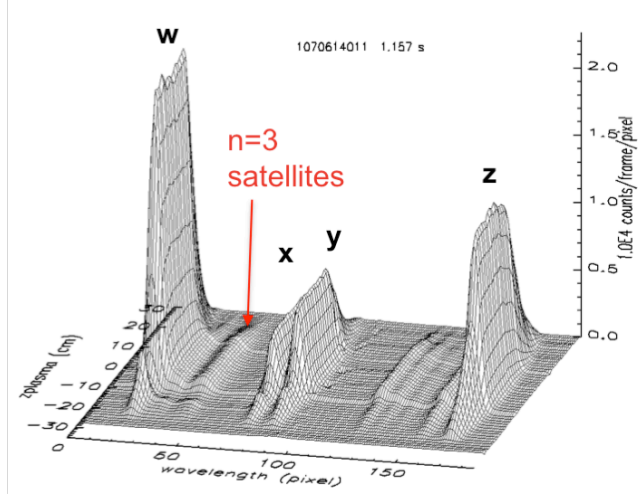


Fig. 2: Spatially resolved spectra of He-like argon from Alcator C-Mod

dielectronic satellite spectra of He-like argon, which were recorded on Alcator C-Mod with a high-resolution x-ray imaging crystal spectrometer that was designed based on the principles explained in Fig. 1. Radial profiles of the ion temperature and toroidal plasma flow velocity on Alcator C-Mod are routinely obtained from a tomographic inversion of those chord-integrated spectra [2].

The concept of our x-ray imaging crystal spectrometer has also been adopted for the design of the x-ray crystal spectrometers on ITER; and a US-ITER Team will be responsible for the design of these spectrometers [3, 4].

II. A new X-ray Line shape Diagnostic for NIF.

The working principle of our x-ray imaging crystal spectrometer can also be applied to the design of a new line-shape diagnostic for precision measurements of the line shape of x-ray

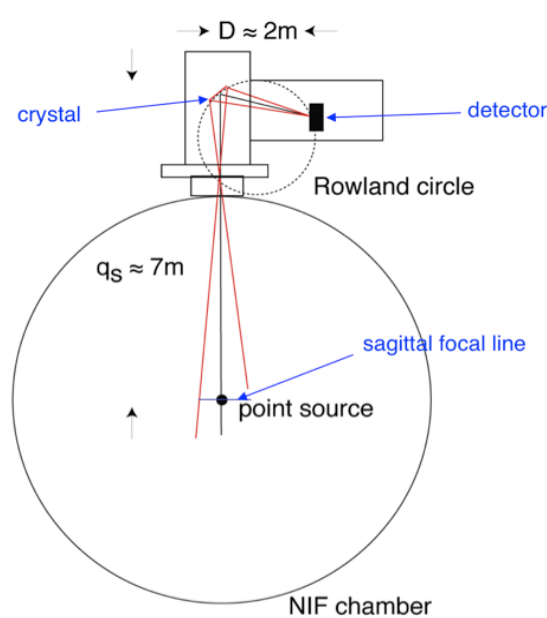


Fig. 3: Line-shape diagnostic for NIF

lines from trace elements in the ICF target at NIF. The objectives of this new diagnostic would be to determine the ion temperature from Doppler broadening and separate the Doppler broadening from Stark broadening effects to also provide a measurement of plasma density [5]. Figure 3 shows a schematic of the NIF target chamber and x-ray imaging crystal spectrometer layout. The radius of curvature of the crystal and the Bragg angle are 2.5 m and 53°, respectively, so that the distances of the crystal from the ICF target and the

detector are 7m and 2m, respectively. Since the detector is outside the target chamber, it can be shielded against neutron and gamma rays. The first measurements will be made with both spatial and temporal integration. However, we will also investigate the feasibility of making spatially resolved measurements in the direction perpendicular to the x-ray diffraction or dispersion plane, as well as the feasibility of making time-resolved measurements with fast imaging detectors, which have been developed at other laboratories. For measurements of spectral line profiles from small ICF targets we would align the spectrometer so that the target is on the center of the sagittal focal line for the central wavelength, λ_0 , of the spectral line of interest, as illustrated in Fig. 4.

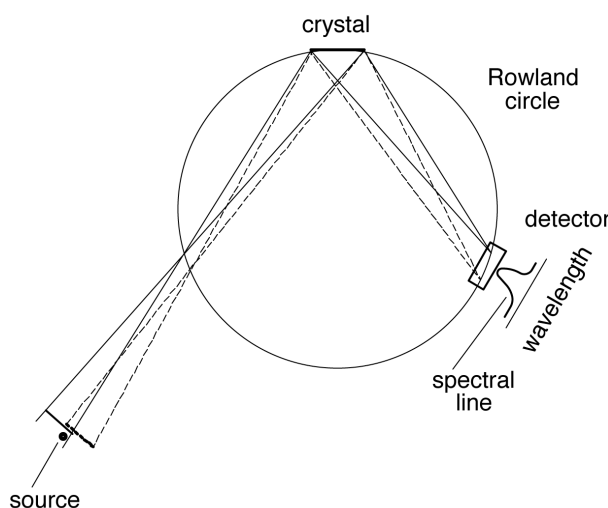


Fig. 5: Lateral shift (not to scale) of sagittal focus with wavelength. The extension of the sagittal focus must be large enough to obtain full spectral coverage.

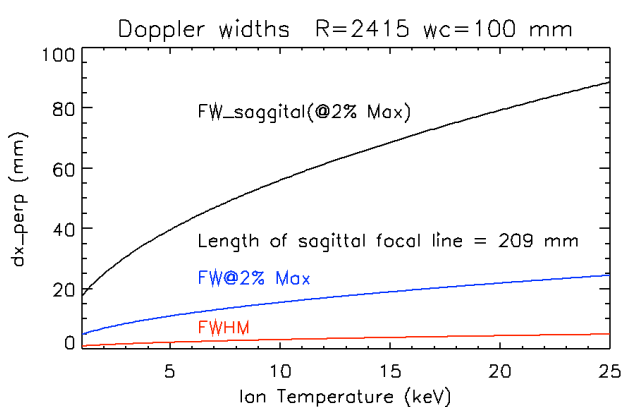


Fig. 6: Line width (red & blue curves) on the detector as function of the ion temperature and wavelength dependent lateral shift of the sagittal focus (black curve) - see text.

The width of the crystal and the resulting width of the sagittal focus must be large enough to obtain full spectral coverage. The red and blue curves in Fig. 6 show the full width at 50% max and 2% max, respectively, on the Rowland circle as a function of the ion temperature. The black curve represents the wavelength dependent lateral shift of the center of the associated sagittal focal line. For a 100mm wide crystal the length of the sagittal line focus that is associated with the central wavelength, λ_0 , would be 209 mm, which is more than sufficient for a full spectral coverage, even for high ion temperatures of 25 keV. According to FLYCHK-code simulations the detector would collect 5×10^3 to 3×10^4 photons of the Kr^{34+} resonance line in 100 ps, with a 100 mm high Ge(555) crystal, from a 25 keV, 100 micron, compressed capsule of electron density 10^{22} cm^{-3} , doped with 0.001% of krypton as trace element.

III. Novel Stigmatic Imaging Schemes.

The astigmatism can be eliminated by the use of two spherical crystals or mirrors, as shown in Fig. 7. The Bragg angle is less than 45° for one crystal and larger than 45° for the other. And the Bragg angles and radii of curvature are properly chosen, so that the real and virtual sagittal images, produced by the two crystals from the respective point sources, coincide [US patent application submitted]. It is thereby possible to obtain stigmatic imaging for almost arbitrary angles of incidence or Bragg angles. This imaging scheme is applicable for a wide spectrum

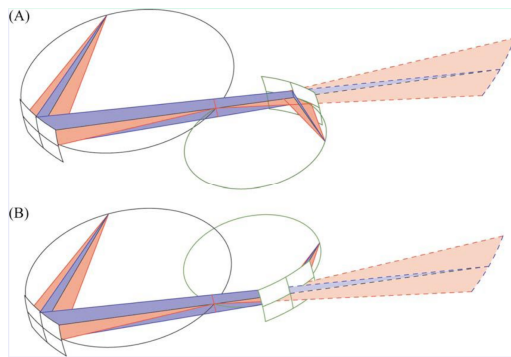


Fig. 7: Novel stigmatic imaging schemes

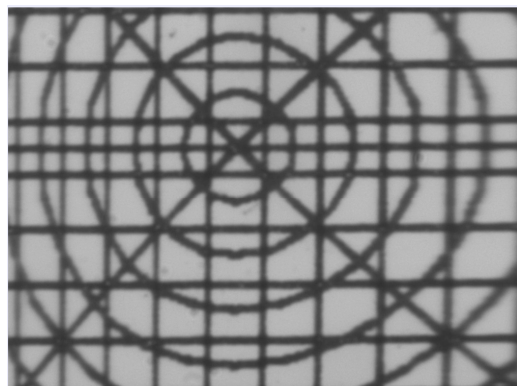


Fig. 8: Stigmatic image of a large (area: $5 \times 5 \text{ mm}^2$) grid obtained with visible light. The line width is 50 microns. The area of the smallest squares is $0.4 \times 0.4 \text{ mm}^2$

of radiation, including microwaves and x-rays; and it is of particular interest for a 2d imaging of NIF plasmas to determine the symmetry of the implosion from emitted x-ray lines or the x-ray continuum radiation. The advantages of these imaging schemes, in comparison to pinhole cameras, are that the crystals would be at a larger distance from the ICF target and that the photon throughput be increased by orders of magnitude, since instead of the pinhole the much larger area of a crystal would serve as the entrance aperture. X-rays are special, since the Bragg condition must be satisfied on both crystals. This condition can only be fulfilled if the Johann aberrations for both crystals are equal and if the scheme (B) of Fig. 7 is used [6]. Tests that verify the concept of these imaging schemes were conducted with visible light - see Fig. 8. Additional tests with x-rays will be performed during this summer.

Acknowledgements.

This work was supported by US Department of Energy Contracts DE-AC02-76-CHO- 3073 and DE-AC53-07NA27344

- [1] M. Bitter et al., *Rev.Sci.Instrum.* **75**, 3660 (2004)
- [2] A. Ince-Cushman et al., *Rev. Sci. Instrum.* **79** 10E302 (2008)
- [3] P. Beiersdorfer et al., *Journal of Physics B* **43**, 144008 (2010)
- [4] K. W. Hill et al., *Rev. Sci. Instrum.* **81** 10E322 (2010); see also K. W. Hill et al. at this conference
- [5] R. J. Tighe, *A Study of Stark Broadening of High-Z Hydrogenic Ion Lines in Dense Hot Plasmas, Ph.D. Thesis Florida Univ., Gainesville*, 77-29, 288, 1977
- [6] M. Bitter et al., *J. Phys. B: At. Mol. Opt. Phys.* **43** 144011 (2010)